J Mater Sci (2008) 43:3643–3648
DOI 10.1007/s10853-008-2580-7

Microstructural and mechanical properties of Sn–Ag–Cu lead-free solders with minor addition of Ni and/or Co

Fangjie Cheng · Hiroshi Nishikawa · Tadashi Takemoto

Received: 1 March 2007 / Accepted: 3 March 2008 / Published online: 23 March 2008
© Springer Science+Business Media, LLC 2008

Abstract The effects of minor additives, that is, Co and Ni, on the microstructural and mechanical properties of Sn–3.0 mass%Ag–0.5 mass%Cu (SAC305) bulk solder were investigated. The addition of Co and/or Ni resulted in microstructural changes of the SAC305 solder, such as the formation of new intermetallic compounds (IMCs) and the refinement of grain size, as well as the suppression of undercooling. The single addition of Co in SAC305 solder resulted in the formation of $CoSn_2$ IMCs and undercooling suppression, whereas the single addition of Ni accelerated the appearance of rod-shaped $(Cu,Ni)_6Sn_5$ IMCs inside the β-Sn dendrites during the solidification process. The dual addition of Co–Ni resulted in refined β-Sn grains and suppression of undercooling, as well as the formation of $CoSn_2$ IMCs. In tensile tests, Co and/or Ni additives had little effect on the tensile strength of SAC305 solder, but obviously suppressed the elongation ratio and reduction of area. During tensile deformation in samples with existing thin plate-like $CoSn_2$ IMCs, micro-cracks or cavities were easily initiated through the interface between $CoSn_2$ and the solder matrix, which was responsible for the decrease of ductility.

Introduction

Lead-free soldering in the electronic industry is showing a global trend toward a lead-free environment. Among the various alloy systems being considered as lead-free solder candidates, Sn–Ag–Cu alloys have been recognized as the most promising because of their relatively low melting temperature (compared with the Sn–Ag and Sn–Cu binary eutectic lead-free solder) and good compatibility with common commercial components [1]. In fact, the hypoeutectic composition Sn–3.0Ag–0.5Cu (SAC305) has become one of the industry standards for lead-free solder alloys in Japan. In a comparison of eutectic or hypereutectic Sn–Ag–Cu alloys during soldering, SAC305 solder does not form large primary Ag_3Sn precipitates, which can deteriorate the ductility of the joints. However, for the hypoeutectic SAC305 solder, the appearance of large β-Sn dendrites reduces the strength and resistance to thermal-mechanical fatigue. In addition, the excessive reactions between lead-free solders and substrate materials are also a problem for the Sn–Ag–Cu lead-free solders [2–4]. It has been proved that the minor element addition is a simple and effective way of modifying the properties of these lead-free solders. Elements such as Zn, Al, Ni, Bi, In, Fe, Co, and rare-earth elements have been utilized to modify the Sn-rich lead-free solder alloys [5–13]. For example, Anderson pointed out that minor substitution of Co for Cu in Sn–3.7Ag–0.9Cu could refine the joint-matrix microstructure and increase the shear strength by an apparent enhanced nucleation of the Cu_6Sn_5 phase [14]. Other research studies have illustrated that Co can suppress the dissolution of the iron tip's Fe plating in the Sn–Ag lead-free solders [15]. Gao et al. [16, 17] pointed out that Co or Ni could result in a great change of the interfacial reaction between the solder and Cu substrate. Furthermore, compared to other elements, Co and Ni are not expensive and are not a byproduct of Pb mining, unlike Bi and Sb, for example. However, most of the experiments reported in the recent literatures focus on the reaction and growth of intermetallic compounds layers at the interface between the

F. Cheng (✉) · H. Nishikawa · T. Takemoto
Joining and Welding Research Institute, Osaka University,
11-1 Mihogaoka, Ibaraki, Osaka 567-0047, Japan
e-mail: chfj@tju.edu.cn

F. Cheng
Materials Science and Engineering School, Tianjin University,
Weijin Road 92, Tianjin 300072, China

solder and substrate, and pay less attention to the microstructural changes and mechanical properties of the solder matrix. In this work, the effects of minor elements, Ni and/or Co, on the microstructural and mechanical properties of SAC305 solder are explored.

Experimental procedures

The nominal compositions of the alloys examined are summarized in Table 1. Seven types of alloys containing various concentrations of Co and Ni additives were prepared. The standard Sn–3.0mass%Ag–0.5mass%Cu was also included as a baseline.

Tensile tests were performed to evaluate the effect of Ni and/or Co addition on the mechanical properties of SAC305 solders. The tensile test specimens were prepared according to JIS Z3198–2, as shown in Fig. 1. The tensile tests were carried out at room temperature at a strain rate of 1×10^{-3}/s. After the tensile tests, the fracture surfaces were observed by the scanning electron microscope (SEM). The microstructure observation was carried out by the optical microscope (OM). The composition of intermetallic compounds (IMCs) was identified by electron probe microanalysis (EPMA). Differential scanning calorimetry (DSC) analysis was carried out to examine the melting and solidification behavior. DSC samples of 15–20 mg were cut from the bulk tensile specimens directly. The heating rate of the DSC tests was 0.33 °C/s, and the solidification process was a natural cooling process. The maximum heating temperature of the DSC test was 350 °C, and the entire process was conducted in N_2 at a flow of 20 mL/min.

Table 1 The nominal chemical compositions of SAC305 solders containing Co and/or Ni

Solders	Elements (mass%)				
	Co	Ni	Ag	Cu	Sn
a: SAC305	–	–	3.0	0.5	Bal.
b: SAC305-0.5Co	0.5	–			
c: SAC305-0.2Co	0.2	–			
d: SAC305-0.1Ni	–	0.1			
e: SAC305-0.05Ni	–	0.05			
f: SAC305-0.5Co–0.1Ni	0.5	0.1			
g: SAC305-0.2Co–0.1Ni	0.2	0.1			
h: SAC305-0.2Co–0.05Ni	0.2	0.05			

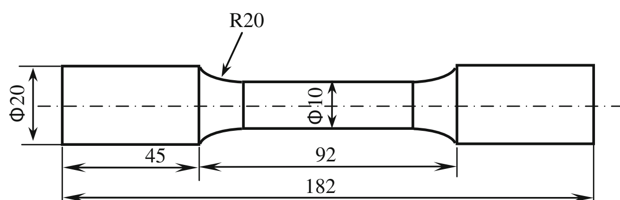

Fig. 1 The shape and dimensions (in mm) of tensile specimen

Results and discussion

Microstructure and solidification behavior

The microstructures of the cast samples with varying Co–Ni content are shown in Fig. 2a–h. These micrographs were taken before the tensile tests and DSC.

The SAC305 alloy shows the typical microstructure of the Sn–Ag–Cu ternary alloy system consisting of β-Sn grains surrounded by the Ag_3Sn–Cu_6Sn_5–Sn eutectic network, as shown in Fig. 2a. As it is a hypoeutectic composition, the volume ratio of the β-Sn phase is very high and its grain size is larger, too. The structure of the eutectic network is superfine and there are no big block-like Ag_3Sn or Cu_6Sn_5 particles in the structure.

After the addition of 0.5mass%Co into SAC305, many block-like intermetallic compounds (IMCs) are observed, as shown in Fig. 2b. The quantitative analysis by EPMA indicated that these IMCs are $CoSn_2$ with a small amount of Cu, as shown in Table 2. These $CoSn_2$ particles are mainly located in the interdendritic eutectic region. Also, even 0.2mass%Co additives result in the formation of $CoSn_2$ IMCs, but the morphology of $CoSn_2$ is different. The photomicrograph in Fig. 2c only shows the cross section of these IMCs, which looked like needles. In fact, they are plate-like in 3-dimension, as shown in the SEM photographs in Fig. 7a

Due to the addition of 0.1mass%Ni, a few short rod-shaped IMCs are generated mainly inside the β-Sn phase, as shown in Fig. 2d. The quantitative analysis indicated that these IMCs are $(Cu,Ni)_6Sn_5$ rather than Ni_3Sn_4 or Ni_3Sn, as listed in Table 2. It implied that the Ni atom could accelerate the formation of Cu_6Sn_5 IMCs and replace some fraction of Cu in the Cu–Sn intermetallic compounds. As we know, the standard Gibbs energy of formation of Cu–Sn is lower than that of Ni–Sn. In addition, the solubility of Ni could stabilize $(Cu,Ni)_6Sn_5$ significantly [18, 19]. SAC305-0.05Ni shows a similar microstructure to SAC305-0.1Ni, as shown in Fig. 2e.

However, the dual addition of Ni and Co causes a more severe modification of the microstructure of SAC305 solder. For example, the 0.5Co–0.1Ni and 0.2Co–0.1Ni additives refine the β-Sn size dramatically, as shown in Fig. 2f and g, while 0.2Co–0.05Ni has a slight effect on the size of β-Sn, as shown in Fig. 2h. Moreover, all of the IMCs in Fig. 2f–h are identified as $CoSn_2$ with a small amount of Ni and Cu solubility, as listed in Table 2. In addition, the quantity of Ni has an impact on the morphology of the $CoSn_2$ IMCs. That is, the

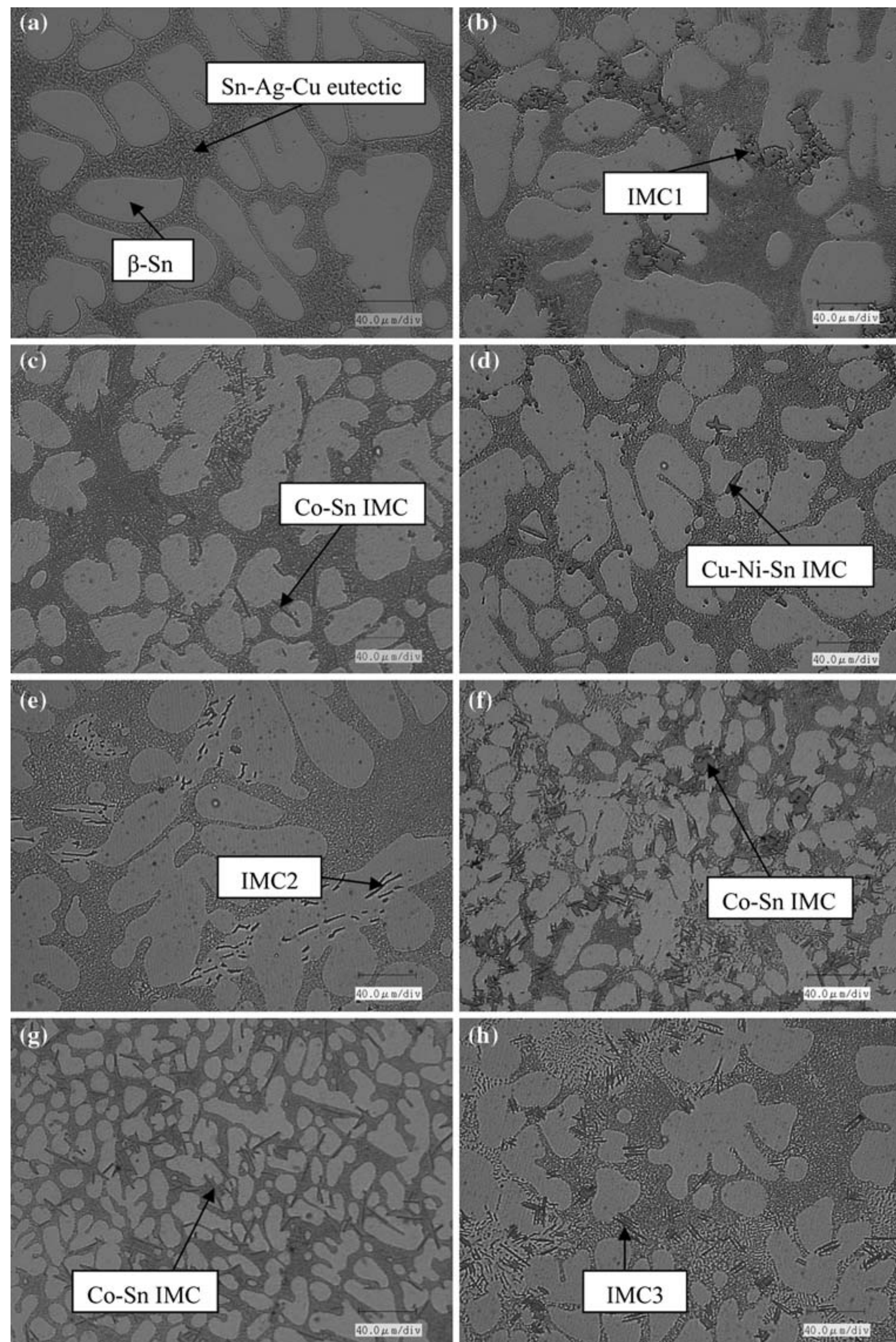

Fig. 2 Photomicrographs of the (**a**) SAC305, (**b**) SAC305–0.5Co, (**c**) SAC305–0.2Co, (**d**) SAC305–0.1Ni, (**e**) SAC305–0.05Ni (**f**) SAC305–0.5Co–0.1Ni, (**g**) SAC305–0.2Co–0.1Ni and (**h**) SAC305–0.2Co–0.05Ni solders

morphology of $CoSn_2$ changes from a plate shape to a stratification structure when the concentration of Ni was changed from 0.1 to 0.05 mass%, as shown in Fig. 2g and h.

The DSC measurement was carried out to assess the solidification behavior of SAC305 alloy doped with Co and/or Ni. Figure 3 depicts the representative DSC curves of the given solders and Table 3 summarizes the undercooling for all solders tested. The heating process of all solders shows a similar tendency, but the cooling process exhibits quite a different tendency. The SAC305 and SAC305-Ni alloys exhibit a single exothermal peak during the cooling process, as well as a large undercooling. It implied that Ni has little effect on the nucleation and solidification of SAC305 solder. On the contrary, all the alloys containing Co or Co–Ni show

Table 2 EPMA quantitative analysis results of the IMCs shown in Fig. 2b, e and h

Elements	IMC1 (in Fig. 2b)		IMC2 (in Fig. 2e)		IMC3 (in Fig. 2h)	
	mass%	at.%	mass%	at.%	mass%	at.%
Sn	80.6	67.5	62.8	47.1	80.8	67.7
Ag	0.0	0.0	0.4	0.3	0.0	0.0
Cu	1.7	2.6	28.4	39.8	1.1	1.7
Co	17.7	29.9	–	–	17.0	28.8
Ni	–	–	8.4	12.8	1.1	1.8
Phase type	$CoSn_2$		$(Cu,Ni)_6Sn_5$		$CoSn_2$	

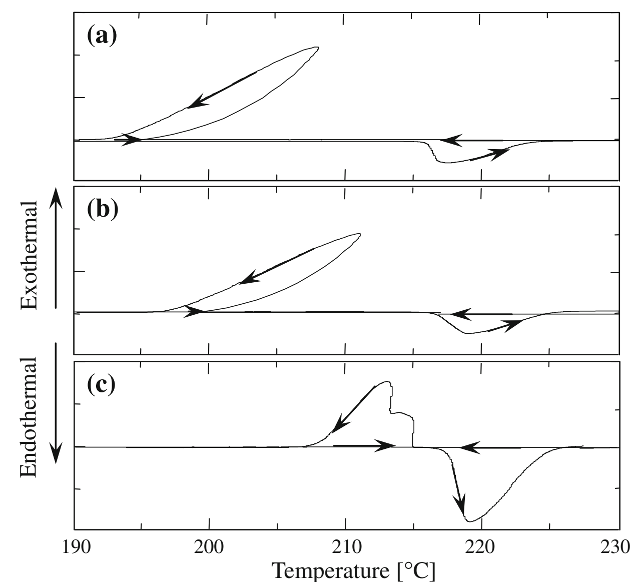

Fig. 3 DSC measurement curves of the (**a**) SAC305, (**b**) SAC305–0.1Ni and (**c**) SAC305–0.2Co solders

dual exothermal peaks. In addition, it is striking that the undercooling is depressed significantly. The undercooling of SAC305-Ni alloys is about 20 °C, which is still comparable to the 23 °C, or so, of SAC305. However, the undercooling of SAC305-Co–(Ni) is only about 4–6 °C, as shown in Table 3. It implied that the Co addition is very effective in suppressing the undercooling of SAC305 solder, whereas the Ni is not very effective. Moreover, only the dual addition of Co–Ni could improve the nucleation power and refine the grain size of primary Sn for the hypoeutectic SAC305 solder; however, the single addition of Co or Ni could not.

Table 3 The undercooling during solidification of various solders

Solders	Undercooling ΔT(°C)
a: SAC305	23
b: SAC305-0.5Co	3.9
c: SAC305-0.2Co	4.0
d: SAC305-0.1Ni	20.1
e: SAC305-0.05Ni	20.2
f: SAC305-0.5Co–0.1Ni	5.9
g: AC-0.2Co–0.1Ni	5.7
h: SAC305-0.2Co–0.05Ni	3.6

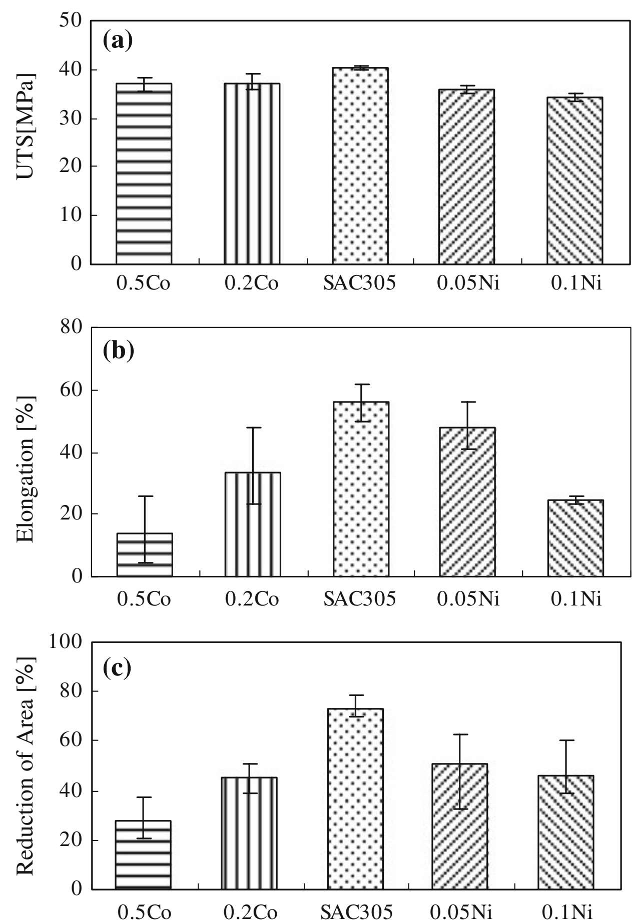

Fig. 4 Tensile properties of SAC305 alloy with single addition of Co or Ni, (**a**) ultimate tensile strength (UTS), (**b**) elongation and (**c**) reduction of area

Tensile test results

The tensile properties of Co-containing or Ni-containing solders are shown in Fig. 4. Apparently, the Co or Ni addition does not significantly impact the ultimate tensile strength (UTS) of SAC305. However, the elongation ratio and reduction of area decline sharply, which indicates that the ductility of SAC305 solder becomes worse after the addition of Co or Ni.

The tensile properties of Co–Ni-containing solders are shown in Fig. 5. As shown in Fig. 5, the dual addition of Co and Ni slightly improves the UTS value of SAC305

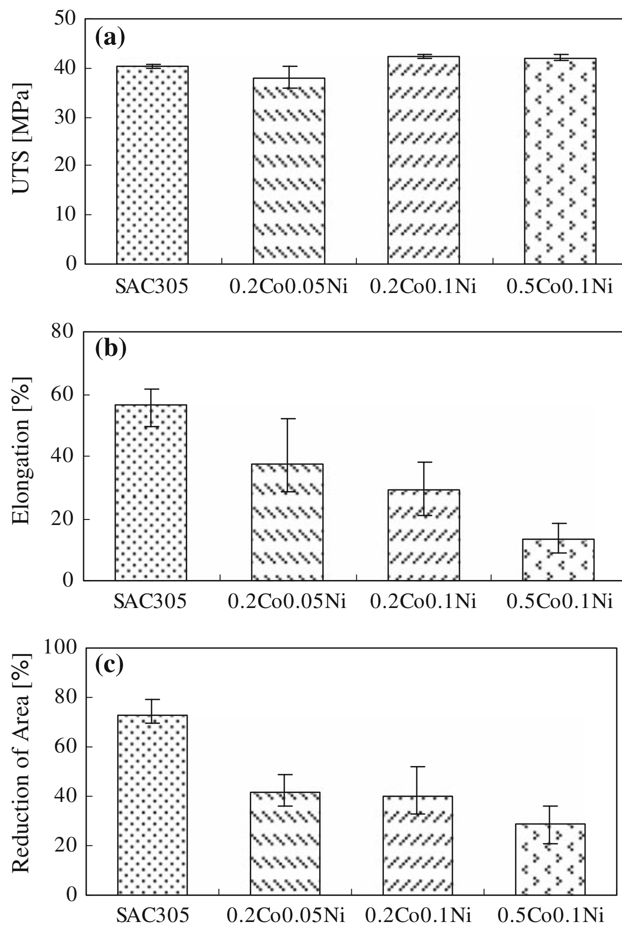

Fig. 5 Tensile properties of SAC305 alloy with dual addition of Co and Ni, (**a**) ultimate tensile strength (UTS), (**b**) elongation and (**c**) reduction of area

solder, except for the SAC305-0.2Co–0.05Ni specimen. However, all the SAC305 solders containing Co–Ni dual additives exhibit worse ductility. The higher content of the additives causes the ductility to deteriorate sharply.

For SAC305-0.2Co–0.1Ni and SAC305-0.5Co–0.1Ni solders, the improved UTS is attributed to the refined microstructure, in particular the β-Sn phase [20]. No remarkable UTS variation is found for SAC305-0.2Co–0.05Ni due to the negligible effect on the β-Sn phase size.

After the tensile tests, the micrographs of the cross sections near the fracture surfaces were examined by OM. The results are shown in Fig. 6a and b for the SAC305-0.2Co and SAC305 solders, respectively. As shown in Fig. 6a, during the tensile process for the solders containing $CoSn_2$ IMCs, most of the cavities or micro-cracks causing the final fracture initiate through the boundary of $CoSn_2$; meanwhile, the tensile deformation of β-Sn grains is slight. For the SAC305 baseline solder, cavities form mainly inside the superfine eutectic network; In addition, the β-Sn grains show heavy tensile deformation, as shown in Fig. 6b. Figure 7 shows the SEM fractograph of SAC305-0.2Co and SAC305 solders after the tensile test. The fracture surface of SAC305-0.2Co shows typical brittle fracture. Thin plate-like $CoSn_2$ precipitates are detectable in the fracture surface. In contrast, the fractograph of the SAC305 solder shows typical plastic fracture, as illustrated in Fig. 7b. So, the existence of $CoSn_2$ precipitates with a jagged shape, which lead to easy initiation of cavities or micro-cracks during tensile deformation is responsible for the decrease of ductility.

Conclusions

The addition of Co and/or Ni resulted in obvious changes in both the microstructural and mechanical properties of Sn–3.0mass%Ag–0.5mass%Cu (SAC305) bulk solder. The single addition of Co in SAC305 solder formed $CoSn_2$ IMCs and suppressed the undercooling during the solidification process, while the single addition of Ni only increased the formation of the rod-shaped $(Cu,Ni)_6Sn_5$ precipitates and very slightly suppressed the undercooling. The single addition of Ni or Co could not refine the β-Sn grains effectively. The dual addition of Co–Ni resulted in not only refined β-Sn grains but also suppression of the undercooling, as well as the formation of $CoSn_2$ IMCs.

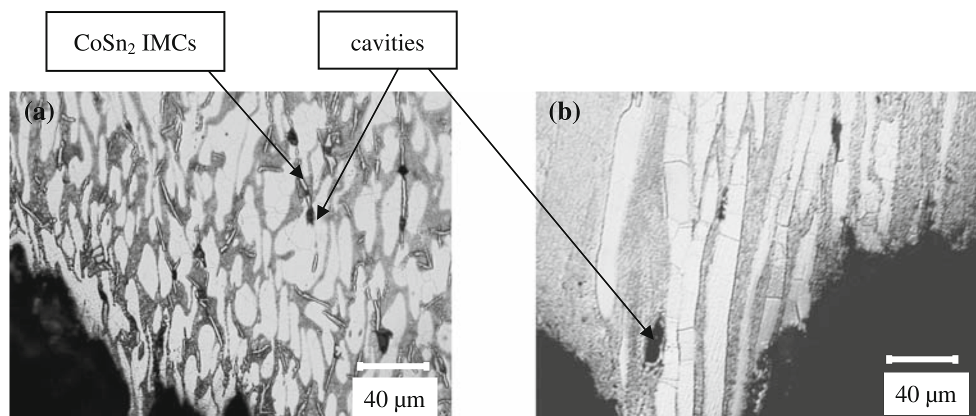

Fig. 6 Cross-sectional micrographs near the fracture surface after tensile testing of the (**a**) SAC305–0.2Co and (**b**) SAC305 solders

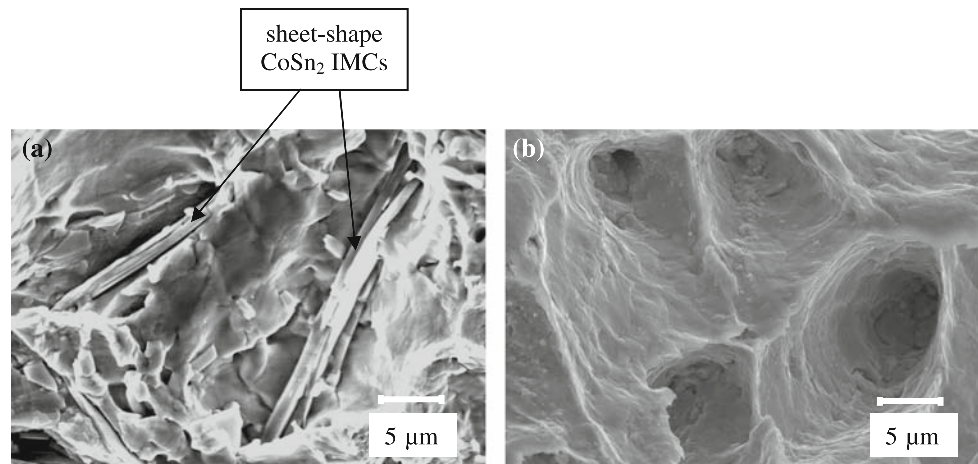

Fig. 7 SEM photographs of the fracture surface after tensile testing of the (**a**) SAC305–0.2Co and (**b**) SAC305 solders

During the tensile tests, Co and/or Ni additives had little effect on the UTS of SAC305 solder; however, the ductility deteriorated notably. The existence of thin plate-like $CoSn_2$ IMCs led to easy initiation of cavities or micro-cracks during tensile deformation, which were responsible for the decrease of ductility.

References

1. Anderson IE, Foley JC, Cook BA, Harringa JL, Terpstra RL, Unal O (2001) J Electron Mater 30:1050
2. Zeng K, Tu KN (2002) Mat Sci Eng R38:55
3. Takemoto T, Takemoto M (2006) Solder Surf Mount Technol 18:20
4. Nishikawa H, Komatsu A, Takemoto T (2005) Mater Trans 46(11):2394
5. Kang SK, Shih DY, Leonard D, Henderson DW (2004) JOM 56:34
6. Kitajima M, Shono T (2005) Microelectron Reliab 45:1208
7. Gourly CM, Nogita K, Mcdonald SD, Nishimora T (2006) Scripta Mater 54:1557
8. Zhao J, Qi L, Wang XM, Wang L (2004) J Alloy Compd 375:196
9. Sharif A, Chan YC (2005) J Alloy Compd 390:67
10. Liu LB, Andersson C, Liu J (2004) J Electron Mater 33:935
11. Kim KS, Huh SH, Suganuma K (2003) Microelectron Reliab 43:259
12. Dudek MA, Sidhu RS, Chawla N (2006) JOM 58:57
13. Wu CML, Yu DQ, Law CMT, Wang L (2004) Mater Sci Eng R44:1
14. Anderson IE, Cook BA, Harringa J, Terpstra RL (2002) J Electron Mater 31:1166
15. Nishikawa H, Komatsu A, Takemoto T (2005) Mater Trans 46:2394
16. Gao F, Takemoto T, Nishikawa H (2006) Mat Sci Eng A420:39
17. Gao F, Takemoto T, Nishikawa H, Komatsu A (2006) J Electron Mater 35:905
18. Laurila T, Vuorinen V, Kivilahti JK (2005) Mat Sci Eng R49:1
19. Lin CH, Chen SW, Wang C-H (2002) J Electron Mater 31:907
20. Anderson IE, Cook BA, Harringa JL, Terpstra RL (2002) JOM 54:26